

# Formulation and Evaluation of an Analytical Model for Composite Box-Beams

Edward C. Smith\* and Inderjit Chopra\*\*

Center for Rotorcraft Education and Research  
Department of Aerospace Engineering  
University of Maryland  
College Park, Maryland

## Abstract

A direct analytical beam formulation is developed for predicting the effective elastic stiffnesses and corresponding load deformation behavior of tailored composite box-beams. Deformation of the beam is described by extension, bending, torsion, transverse shearing, and torsion-related out-of-plane warping. Evaluation and validation of the analysis is conducted by correlation with both experimental results and detailed finite element solutions. The analysis is evaluated for thin-walled composite beams with no elastic coupling, designs with varying degrees of extension-torsion and bending-shear couplings, and designs with bending-torsion and extension-shear coupling. The analysis performed well over a wide range of test cases, generally predicting beam deformations within 10% of detailed finite element solutions. The importance of three non-classical structural phenomenon is systematically investigated for coupled composite beams. Torsion-related out-of-plane warping can substantially influence torsion and coupled torsion deformations; twist of a symmetric layup box-beam under a tip bending load can increase up to a 200% due to warping. Couplings associated with transverse shear deformations can significantly alter the elastic response of tailored composite box-beams; effective bending stiffness of highly coupled anti-symmetric layup beams can be reduced more than 30%. Two-

dimensional in-plane elastic behavior of the plies is also very important to the accuracy of composite box-beam analysis; load deflection results for anti-symmetric layup beams can be altered by 30-100% by not accounting for this elastic behavior.

## Nomenclature

$c$	= chord or width of box-beam cross-section (outer)
$d$	= depth of box-beam cross-section (outer)
$f$	= transverse in-plane strain function term
$s$	= contour coordinate
$t$	= thickness of either ply or box-beam wall
$u$	= axial deformation due to extension
$v$	= horizontal deformation due to bending
$w$	= vertical deformation due to bending
$x$	= beam coordinate in axial (spanwise) direction
$A$	= enclosed area of cross-section
$E$	= elastic modulus of composite ply
$F$	= net axial force on cross-section
$G$	= in-plane shear modulus (ply or laminate)
$L$	= beam length
$M$	= net bending moment on cross-section
$Q$	= net shear force on cross-section
$T$	= net torque on cross-section
$U$	= total axial deformation
$V$	= total horizontal deformation
$W$	= total vertical deformation
$\alpha$	= non-dimensional warping parameter

\* *Minta Martin Fellow, Student Member AIAA, AHS*

\*\* *Professor, Associate Fellow AIAA, Member AHS*

- $\beta$  = non-dimensional warping parameter  
 $\gamma$  = transverse shear strain in cross-section  
 $\delta$  = warping function parameter  
 $\epsilon$  = strain component in beam wall  
 $\zeta$  = cross-section coordinate  
 $\eta$  = cross-section coordinate  
 $\lambda$  = torsion-related warping function  
 $\theta$  = ply orientation angle  
 $\nu$  = Poisson's ratio of composite ply (major)  
 $\sigma$  = stress component in beam wall  
 $\phi$  = twist angle  
 $\mathbf{x}$  = deformation vector  
 $\mathbf{F}$  = load vector  
 $\mathbf{A}$  = laminate in-plane stiffness matrix  
 $\mathbf{K}$  = beam stiffness matrix  
 $\mathbf{Q}$  = ply stiffness matrix

### Subscripts

- $h$  = horizontal walls  
 $v$  = vertical walls  
 $x$  = axial direction of beam  
 $y$  = transverse (horizontal) direction of beam  
 $z$  = transverse (vertical) direction of beam  
 $L$  = longitudinal direction of ply  
 $T$  = transverse direction of ply  
 $eff$  = effective for in-plane shear modulus  
 $ply$  = ply for thickness

### Superscripts

- $o$  = cross-section transverse shear strain  
 $'$  = axial differentiation or modified matrix term

## I. Introduction

### *Background*

The benefits of advanced composite materials and box-beam constructions have been widely recognized by the aerospace community. Many primary structural components such as helicopter blades and aircraft wing spars now feature composite box-beam designs. These composite designs are lightweight, have enhanced fatigue and damage behavior, and offer innovative and cost-effective fabrication characteristics, however, the inherent tailorability of composite structures has not been fully taken advantage of. In particular, the elastic couplings between various modes of deformation are typically not exploited in composite designs. These couplings, such as bending-torsion or extension-torsion, arise due to the anisotropic or directional nature of fibrous composites. One of the most dramatic applications of

this technology is the use of bending-torsion coupled composite structure to prevent divergence of the forward swept wing [1]. Composite designs which exhibit various couplings appear to have great potential for use in helicopter blades and tilt-rotor blades to reduce vibration, enhance aeroelastic stability, and improve aerodynamic efficiency [2-5]. Successful application of tailored composite box-beam structures requires the development and validation of new analytical tools which are both sufficiently accurate and computationally efficient.

Recent efforts toward the creation of new analytical tools for composite beams have led to the development of several finite element based methods [6-18]. The finite element models provide varying degrees of analytical flexibility depending on the level of computational effort. Detailed finite element formulations have been used to capture a variety of non-classical phenomenon in composite beams and blades. For example, Borri et. al. [7,8], Bauchau and Hong [9-11], and Stemple and Lee [12-14] have investigated the effects of warping and large displacements using specially designed beam finite elements or combinations of isoparametric elements. Kosmatka and Friedmann [15-17] have also studied twisted composite blades using isoparametric elements. Although these methods are quite powerful, a certain amount of physical insight is often sacrificed in the formulation and implementation of large scale discretized numerical solutions. Detailed finite element techniques can become impractical if implemented in aeroelastic or optimization analyses.

A number of direct analytical methods have also been formulated for thin-walled composite beams [2-4, 19-32]. Reissner and Tsai [19] developed shell analysis for bending stretching and twisting of composite shell structures. Mansfield and Sobey [20] developed a simple thin-walled contour analysis and introduced the concept of the aeroelastically tailored composite helicopter blade. Using a simple composite beam model, Hong and Chopra [2-3] formulated comprehensive analysis for aeroelastic stability of advanced composite rotor systems. Panda and Chopra [4] extended this analysis from hover to the forward flight condition, and demonstrated the potential for composite tailoring to increase aeroelastic stability and reduce blade vibration. Rehfield [21] developed a thin-walled contour analysis for tailored composite beams. Rehfield, Hodges, Atilgan, and Nixon have applied this formulation to a variety of beam problems. Most of this work has been for beams with

extension-torsion and bending shear couplings [22-23]. Bauchau has also developed a thin-walled contour formulation using a refined approach to warping [24]. Variations of this work have been incorporated into a finite element method [9-11]. Bicos and Springer [25] investigated the minimum weight design of a semi-monocoque (stringers and webs) composite box-beam using a reduced plate model. Libove and Chang [26-27] have also developed a thin-walled contour analysis which is similar to the work of Mansfield and Sobey [20]. Klang and Kuo [28] recently developed a method using plates and corner springs to model the composite box-beam. Rand [29-30] has investigated rotating composite beams using a structural model similar to that of Hong and Chopra. Rand's analysis uses a more refined treatment of warping and a Galerkin approach to calculate dynamic blade response. Minguet and Dugundji [31-32] used a reduced plate formulation to investigate coupled composite beams. The main focus of this experimental and analytical study was on solid section beams under large deflections.

These direct analytical methods are typically based on combinations of beam theory and classical lamination theory. Certain simplifying assumptions are made in order to obtain governing differential equations without discretizing the entire problem. In some cases the governing equations can then be solved directly [21-23, 26-27]. Variational principles can also be used to determine approximate solutions [24,25,28-32]. In addition to computational simplicity and speed (relative to detailed finite element models), direct analytical formulations can provide valuable cause-effect relationships and enhanced physical understanding of non-classical phenomenon and elastic coupling effects. Direct analytical models are also very useful in evaluating the effects of composite design changes on overall system performance. Examples of such studies were the investigations of ply orientation on the aeroelastic stability of composite helicopter blades [2-4]. Structural optimization is also an area where direct analytical formulations can be particularly appealing.

Despite the increased appearance of the aforementioned finite element and direct analytical methods during the past decade, the structural behavior of composite box-beams is not yet thoroughly understood. Some of the methods have not been fully developed and most of the methods have not been thoroughly validated for general composite designs. In particular, there have been

some selected validation studies dealing with extension-twist coupled beam structures [18, 22], however, there has been very little thorough validation of analyses for bending-torsion coupled structures and structures with variations in stiffness around the cross-section. Validation is especially important for direct analytical methods since the major simplifying assumptions can effect the applicability limits of the model. Many of the methods which have been previously developed, especially the direct analytical methods, do not address all of the non-classical effects, consequently, the importance of many non-classical structural phenomenon associated with composite beam constructions has not been clearly established, or quantified.

### *Scope and Description of Present Research*

The objectives of this study are: (1) to develop a direct analytical method for predicting the effective elastic stiffnesses and corresponding load deformation behavior of composite box-beams, (2) to thoroughly validate and evaluate the analytical method, and (3) to apply the new analysis to examine the importance of non-classical structural phenomenon. This analytical capability and understanding is especially important to the dynamic analyses of tailored composite helicopter rotor blades.

A systematic approach is taken to develop both a qualitative and quantitative understanding of the composite box-beam behavior. Special consideration is given to modeling the effects of anisotropic elasticity, laminated construction, torsion-related warping, and transverse shear. Critical evaluation of the analytical method is carried out by correlating the analytical results with both experimental results and finite element solutions. The analysis is then applied to investigate non-classical phenomenon such as warping, transverse shear, and transverse in-plane elasticity.

The deformation of the box-beam is described by extension, bending, twisting, shearing, and torsion-related out-of-plane warping. The composite walls of the rectangular box-beam are represented as four laminated plates which are built up from layers of orthotropic plies. Unlike box-beams constructed using isotropic materials, the elastic properties of the laminated composite box-beam designs generally vary both through the thickness and around the contour of the beam cross-section. This unique

distribution of stiffness enhances the tailorability of composite structures. By varying the ply layup within the beam walls (fiber orientation angle, stacking sequence, ply material, etc.) structural designers can create elastic couplings between deformations such as extension and torsion, bending and torsion, or even bending and shearing of the beam.

Many of the current direct analytical methods for composite beams are based heavily on thin walled beam theory [21-23,26-27]. Variations in stresses, strains and elastic properties through the thickness of the laminated beam walls must be treated in an approximate manner which can break down as wall thickness increases. The present analysis is developed without much dependence on thin walled beam theory. Formulation of the analysis in terms of a two-dimensional cross-section, instead of an infinitely thin contour enables stresses, strains, and elastic properties to vary through the thickness of the beam walls in a manner consistent with the true laminated nature of the composite structure. This analytical detail is very useful in studying non-classical phenomenon such as warping, and in-plane elasticity.

Governing differential equations for the extension, bending, torsion, and shearing of the beam are derived using a Newtonian approach. This method, in which applied forces and moments over the cross-section are reacted by stresses within the beam walls, is very commonly applied in formal elasticity solutions. Variational or energy methods can also be used to derive the governing beam equations. The variational approach is very useful for complex problems involving non-linear behavior.

Validation studies are carried out for composite designs with no coupling, designs with varying degrees of extension-torsion and bending-shear coupling, as well as designs with varying degrees of bending-torsion and extension-shear coupling. Performance of the analysis at high ply orientation angles (up to 45 degrees) is also investigated. The analysis is evaluated by correlation with both detailed finite element solutions and experimental results.

The treatment of warping must receive special attention for composite structures [2-4,7-18,21-24,29-30]. The distribution of stiffness throughout the beam cross-section can significantly influence on the shape of the out-of-plane warping deformation,

consequently, the accuracy of composite beam formulations can be significantly effected by the manner in which warping is treated. It is important to note that the modelling of warping can become quite involved in finite element formulations, therefore, a great deal of effort has gone into treating warping on a level which is both simple and yet sufficiently accurate.

The effects of transverse shear deformation of the cross-section are also investigated. Transverse shear can become very important for even slender composite box-beams depending on the particular ply layup and dimensions of the beam cross-section [22,23]. In the present model, transverse shear of the cross-section is investigated, however, transverse shear of the composite beam walls is assumed negligible. Inclusion of this effect becomes more necessary as the thickness of the beam walls increases.

Another key element of the composite beam formulation is the manner in which two-dimensional anisotropic elastic behavior of the beam walls is captured by one-dimensional beam theory. In other words, Poisson's effect can become more significant for certain composite designs. Both the strain-displacement and stress-strain relations are important to this critical issue. Methods for bridging this analytical gap are investigated and critically evaluated.

## II. Formulation of Analysis

The box-beam geometry and coordinates are shown in Figure 1. The cross-section axis origin is at the center of the beam section.

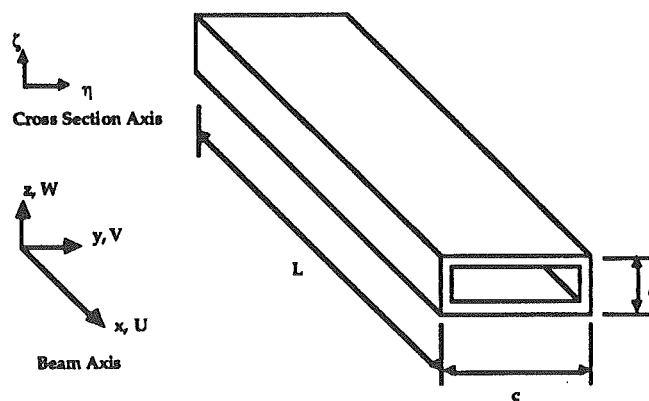


Figure 1. Box-Beam Configuration and Coordinates

The deformation of the beam cross-section is described by stretching, bending, twisting, shearing, and warping. These assumptions yield displacements of the form

$$U = u(x) - \eta \left( v'(x) - \gamma_{xy}^0(x) \right) - \zeta \left( w'(x) - \gamma_{xz}^0(x) \right) - \lambda \phi'(x) \quad [1a]$$

$$V = v(x) - \zeta \phi(x) \quad [1b]$$

$$W = w(x) + \eta \phi(x) \quad [1c]$$

The underlined terms represent the warping of the cross-section. Note that the term "warping" represents the out-of-plane axial displacement of the cross-section due to torsional deformation. This is commonly referred to as torsion-related warping. Warping can play a very significant role in the torsional behavior of a thin-walled beam [33-36]. In the present analysis, the thin-walled beam theory approach described in Megson [36] is modified to determine the shape of the warping deflections for a composite box-beam. This shape, or warping function, is then transformed from contour form to two-dimensional cross-sectional form. The warping function is then carried through the entire analysis, from the initial kinematic relations to the effective stiffnesses of the beam cross-section. This approach is particularly useful for studying the quantitative effects of warping on the elastic behavior of the box-beam structure. It is important to note that this is the only point in the analysis where the cross-section is treated on the contour level of thin-walled beam theory.

The warping function is defined along the contour as

$$\lambda(s) = 2A \left( \frac{\delta_{os}}{\delta} - \frac{A_{os}}{A} \right) \quad [2]$$

The enclosed area of the cross-section,  $A$ , is

$$A = cd \quad [3]$$

and other contour parameters defined as

$$\delta = \int_S \frac{ds}{G(s)t(s)} \quad [4]$$

$$\delta_{os}(s) = \int_0^s \frac{ds}{G(s)t(s)} \quad [5]$$

and  $A_{os}$  is the area swept out by a generator, with origin at the box-beam center, from  $s=0$  to  $s=s$  on the contour.

After evaluating all line integrals around the cross-section, the contour warping function,  $\lambda(s)$ , can be simply transformed into the two-dimensional cross-sectional form

$$\lambda(\eta, \zeta) = \beta \eta \zeta \quad [6]$$

with  $\beta$  given by

$$\beta = \frac{(1 - \alpha)}{(1 + \alpha)} \quad [7]$$

and  $\alpha$  given by

$$\alpha = \left( \frac{c}{d} \right) \left( \frac{t_v}{t_h} \right) \left( \frac{G_v}{G_h} \right) \quad [8]$$

At this point, an effective in-plane shear stiffness for the composite beam walls must be specified. Consider a single beam wall as a laminated plate. The relations between in-plane stress resultants  $N_{xx}$ ,  $N_{yy}$ , and  $N_{xy}$  and in-plane strains  $\epsilon_{xx}$ ,  $\epsilon_{yy}$ , and  $\epsilon_{xy}$  are

$$\begin{Bmatrix} N_{xx} \\ N_{yy} \\ N_{xy} \end{Bmatrix} = \begin{bmatrix} A_{11} & A_{12} & A_{16} \\ A_{12} & A_{22} & A_{26} \\ A_{16} & A_{26} & A_{66} \end{bmatrix} \begin{Bmatrix} \epsilon_{xx} \\ \epsilon_{yy} \\ \epsilon_{xy} \end{Bmatrix} \quad [9a]$$

with,

$$A_{ij} = \sum_{n=1}^{\text{\# of plies}} \bar{Q}_{ij}^{(n)} t_{ply}^{(n)} \quad [9b]$$

The elements of the ply stiffness matrix,  $\bar{Q}$ , are defined in texts discussing macromechanical behavior of composite plies [37]. These stiffness coefficients are functions of ply orientation angle  $\theta$ . If transverse in-plane stress resultant  $N_{yy}$  is assumed small for beam structures, the stiffness matrix simplifies to

$$A' = \begin{bmatrix} \left( A_{11} - \frac{(A_{12})^2}{A_{22}} \right) & \left( A_{16} - \frac{A_{12}A_{26}}{A_{22}} \right) \\ \left( A_{16} - \frac{A_{12}A_{26}}{A_{22}} \right) & \left( A_{66} - \frac{(A_{26})^2}{A_{22}} \right) \end{bmatrix} = \begin{bmatrix} A'_{11} & A'_{16} \\ A'_{16} & A'_{66} \end{bmatrix} \quad [10]$$

An effective in-plane shear stiffness can now be defined by considering the shear strain,  $\epsilon_{xy}$ , which results from an applied shear force resultant  $N_{xy}$

$$G_{\text{eff}} = t_{\text{wall}} \left( A'_{66} - \frac{(A'_{16})^2}{A'_{11} A'_{66}} \right) \quad [11]$$

This approach captures the effects of elastic coupling in the anisotropic plies in a practical approximate manner.

Strains are determined by differentiating these displacement terms. At this point, the walls of the box-beam are assumed to be relatively thin; therefore, only axial and in-plane shear strains are considered non-negligible. The resulting strains are

$$\epsilon_{xx} = u' - \eta(v'' - \gamma_{xy}^0) - \zeta(w'' - \gamma_{xz}^0) - \lambda\phi'' \quad [12]$$

$$\epsilon_{x\zeta} = \left( \eta - \frac{\partial\lambda}{\partial\zeta} \right) + \gamma_{xz}^0 \quad [13]$$

in the vertical walls, and

$$\epsilon_{xx} = u' - \eta(v'' - \gamma_{xy}^0) - \zeta(w'' - \gamma_{xz}^0) - \lambda\phi'' \quad [12]$$

$$\epsilon_{x\eta} = - \left( \zeta + \frac{\partial\lambda}{\partial\eta} \right) + \gamma_{xy}^0 \quad [14]$$

in the horizontal walls.

In standard beam theory, the transverse in-plane normal strain,  $\epsilon_{yy}$ , will not enter the formulation. This is a natural consequence of the one-dimensional nature of beam theory itself. However, when the walls of the box-beam are made of laminated composite material plies, transverse in-plane normal stresses and strains can become quite important. The anisotropic elastic characteristics of composite plies can result in highly two-dimensional elastic behavior. This becomes more apparent upon considering the stress-strain relationship for a single ply of composite material. These elastic constitutive relations are

$$\begin{Bmatrix} \sigma_{xx} \\ \sigma_{yy} \\ \sigma_{xy} \end{Bmatrix} = \begin{bmatrix} \bar{Q}_{11} & \bar{Q}_{12} & \bar{Q}_{16} \\ \bar{Q}_{12} & \bar{Q}_{22} & \bar{Q}_{26} \\ \bar{Q}_{16} & \bar{Q}_{26} & \bar{Q}_{66} \end{bmatrix} \begin{Bmatrix} \epsilon_{xx} \\ \epsilon_{yy} \\ \epsilon_{xy} \end{Bmatrix} \quad [15]$$

Coupling between extension and in-plane shear within the composite ply is the source of the elastic couplings in composite structures. For unidirectional fiber plies at orientation angles of 0 or 90 degrees, coupling stiffness terms  $\bar{Q}_{16}$  and  $\bar{Q}_{26}$  are zero.

Note that subscript y would correspond to  $\eta$  in the horizontal walls and  $\zeta$  in the vertical walls. The specific manner in which the two-dimensional nature of the composite walls is captured by one-dimensional beam theory is another important issue in composite box-beam analysis. Three different methods have been examined to handle this problem. The most refined (and effective) method is explained at this point.

In order to keep the formulation within the context of beam theory, the following conditions are imposed on the transverse in-plane normal stresses

$$\iint \sigma_{yy} dA = 0 \quad [16a]$$

$$\iint \sigma_{yy} \eta dA = 0 \quad [16b]$$

$$\iint \sigma_{yy} \zeta dA = 0 \quad [16c]$$

This is equivalent to setting the net in-plane force and in-plane bending moments to be zero. Transverse in-plane normal strain,  $\epsilon_{yy}$ , is determined to satisfy these conditions. In order to prescribe  $\epsilon_{yy}$ , this strain must be written in general form as a continuous function within the cross-section.

$$\epsilon_{yy} = f_u u' + f_v v'' + f_w w'' + f_{\gamma_{xy}} \gamma_{xy}^0 + f_{\gamma_{xy}} \gamma_{xy}^0 + f_{\phi} \phi' + f_{\phi} \phi'' \quad [17]$$

Where the coefficients of the deformations are linear functions within the cross-section. For example

$$f_u = a_0 + a_1 \eta + a_2 \zeta \quad [18a]$$

$$f_v = b_0 + b_1 \eta + b_2 \zeta \quad [18b]$$

The constants  $a_0$ ,  $a_1$ ,  $a_2$ , etc. are determined from the three conditions on the in-plane stresses. Once the in-plane strain function is fully determined in terms of elastic constants and cross-section geometry,  $\epsilon_{yy}$  can

be removed from the constitutive relations by substitution. This procedure is a more refined version of the procedure used previously during the determination of the effective in-plane shear modulus  $G_{eff}$ .

By substituting the strain-displacement relations into the stress-strain relations, the stresses within the beam walls can be related to the displacements of the beam cross-section. The net forces and moments acting over the cross-section can be related to the stresses in the beam walls by equilibrium as follows

$$F = \iint \sigma_{xx} dA \quad [19a]$$

$$Q_y = \iint \sigma_{x\eta} dA \quad [19b]$$

$$Q_z = \iint \sigma_{x\zeta} dA \quad [19c]$$

$$T = \iint \left[ \left( \eta - \frac{\partial \lambda}{\partial \zeta} \right) \sigma_{x\zeta} - \left( \zeta + \frac{\partial \lambda}{\partial \eta} \right) \sigma_{x\eta} \right] dA + \frac{\partial}{\partial x} \left[ \iint \lambda \sigma_{xx} dA \right] \quad [19d]$$

$$M_y = - \iint \sigma_{xx} \zeta dA \quad [19e]$$

$$M_z = - \iint \sigma_{xx} \eta dA \quad [19f]$$

All of these expressions are quite natural except for the distribution of shear on the cross-section,  $T$ . As demonstrated by Brunelle [38], torsion-related out-of-plane warping effects the net torque on the section. This effect can have considerable influence on elastic couplings for composite box-beams.

Since the stresses are known in terms of the displacements, the governing differential equations relating cross-sectional loads (forces and moments) to cross-sectional displacements (stretching, bending, twisting, shearing, and warping) are derived. In matrix form, this can be written

$$F = Kx \quad [20]$$

With  $F$  and  $x$  given by

$$F = \{F \ Q_y \ Q_z \ T \ M_y \ M_z\}^T \quad [21]$$

$$x = \{u' \ \gamma_{xy}^o \ \gamma_{xz}^o \ \phi' \ (w'' - \gamma_{xz}^o) \ (v'' - \gamma_{xy}^o)\}^T \quad [22]$$

The specific elements of  $K$  which apply to the present analysis are given in Appendix A.

From this set of governing equations, beam displacements can be determined if the applied forces and moments are known.

The present analytical formulation can further be used to formulate approximate solutions using finite element or other variational methods.

### III. Evaluation and Validation of Analysis

Results of the analytical formulation are validated by correlation with experimental data and detailed finite element formulation results. For validation, three classes of composite design were selected. Beam specimens which are fabricated and tested include cross-ply layup designs, symmetric layup designs, and anti-symmetric layup designs. In order to clarify terminology, the different beam configurations are shown in Figure 2.

Cross-ply layup beams do not display any elastic couplings. Symmetric layup beams display bending-torsion coupling and extension-shear coupling. Anti-symmetric layup beams display extension-twist coupling and bending-shear coupling. For these three classes of composite design, many of the elastic couplings will not exist. The simplified forms of the governing differential equations are given in Appendix B. Varying levels of coupling behavior are generated in different beam specimens by varying off-axis ply angles from 15 degrees to 45 degrees. Physical geometry of the beam specimens is given in Table 1. A summary of the different composite designs and loading conditions is presented in Table 2.

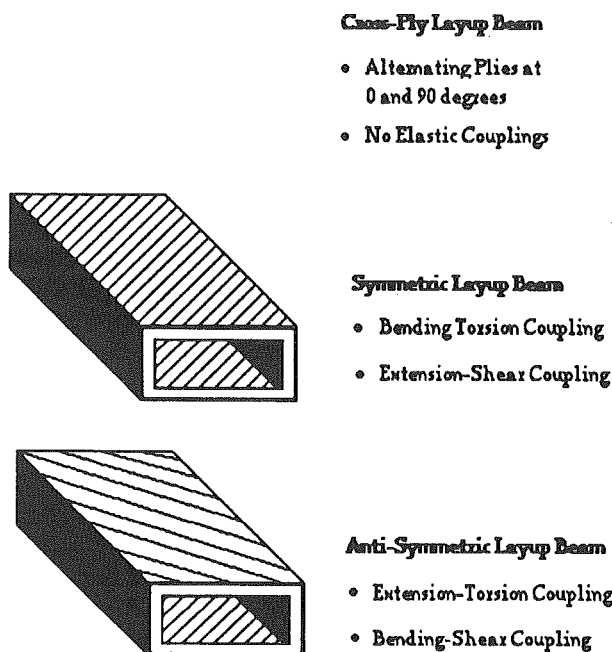


Figure 2. Composite Layup Designations

### Correlation with Experimental Results

The experimental data has been furnished by in-house studies conducted by Chandra et al. at the University of Maryland [39, 40]. An autoclave molding technique is used to fabricate the composite box beams from unidirectional Graphite/Epoxy prepreg plies (Hercules AS4/3501-6). The elastic properties for this material are given in Table 3. After the prepreps are cut to desired size and ply orientation using custom designed templates, they are laid up by hand onto an aluminum mold. The layup is then prepared in a vacuum bag, cured in the autoclave facility, and removed from the aluminum mold. Using the apparatus shown in Figure 3, cantilevered beam specimens were subjected to extensional tip loads, tip torques, and transverse tip bending loads (bending about y axis in all bending cases). A series of mirrors was fixed along the beam span, and bending slope and twist angle of the composite box-beams was measured using a laser optics system.

Dimensions (inches)	L / d = 56	L / d = 29
L	30	30
d	0.537	1.025
c	0.953	2.060
Ply Thickness	0.005	0.005
Wall Thickness (6 Ply)	0.030	0.030

Table 1. Physical geometry of Box-Beam Specimens

### Correlation with Finite Element Results

Analytical results are also correlated with the finite element formulation developed by Stemple and Lee [12-14]. This formulation uses a shear flexible beam element with warping displacements parallel to the deformed beam axis. The fully coupled warping displacements are then superimposed over the cross-section.

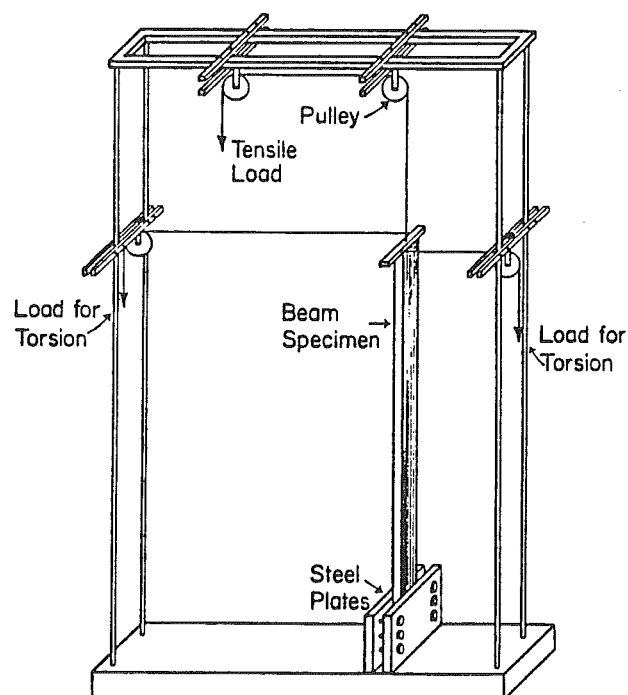


Figure 3. Experimental Test Apparatus



	L/d	Top & Bottom	Sides	Loading
Cross-Ply Layups	29	(0/90) <sub>3</sub>	(0/90) <sub>3</sub>	Bending
	29	(0/90) <sub>3</sub>	(0/90) <sub>3</sub>	Torsion
	56	(0/90) <sub>3</sub>	(0/90) <sub>3</sub>	Bending
Anti-Symmetric Layups	56	(15) <sub>6</sub>	(15) <sub>6</sub>	Extension
	56	(15) <sub>6</sub>	(15) <sub>6</sub>	Torsion
	56	(15) <sub>6</sub>	(15) <sub>6</sub>	Bending
	56	(0/30) <sub>3</sub>	(0/30) <sub>3</sub>	Extension
	56	(0/30) <sub>3</sub>	(0/30) <sub>3</sub>	Torsion
	56	(0/30) <sub>3</sub>	(0/30) <sub>3</sub>	Bending
	56	(0/45) <sub>3</sub>	(0/45) <sub>3</sub>	Extension
	56	(0/45) <sub>3</sub>	(0/45) <sub>3</sub>	Torsion
	56	(0/45) <sub>3</sub>	(0/45) <sub>3</sub>	Bending
Symmetric Layups	29	(15) <sub>6</sub>	(15/-15) <sub>3</sub>	Torsion
	29	(30) <sub>6</sub>	(30/-30) <sub>3</sub>	Torsion
	29	(45) <sub>6</sub>	(45/-45) <sub>3</sub>	Torsion
	56	(15) <sub>6</sub>	(15/-15) <sub>3</sub>	Bending
	56	(15) <sub>6</sub>	(15/-15) <sub>3</sub>	Torsion
	56	(30) <sub>6</sub>	(30/-30) <sub>3</sub>	Bending
	56	(30) <sub>6</sub>	(30/-30) <sub>3</sub>	Torsion
	56	(45) <sub>6</sub>	(45/-45) <sub>3</sub>	Bending
	56	(45) <sub>6</sub>	(45/-45) <sub>3</sub>	Torsion

Table 2. Summary of Validation Cases


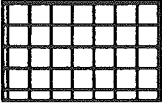
	Hercules AS4/3501-6 Unidirectional Graphite/Epoxy	T650-42/ERLX 1925-2 Cloth Graphite/Epoxy
		
E <sub>L</sub> (msi)	20.59	11.65
E <sub>T</sub> (msi)	1.42	11.65
G <sub>LT</sub> (msi)	0.87	0.82
ν <sub>LT</sub>	0.42	0.05

Table 3. Ply Material Properties (t<sub>ply</sub> = 0.005 in)

Some correlation is also carried out using a three-dimensional solid element model developed by Kim and Lee [41]. For the slender box-beams considered in the present analysis, the modified beam and solid elements yielded basically identical results; therefore, most finite element correlations were made using the modified beam element.

All correlation results are presented for "unit" applied loads or torques. Experimental deflections remain in the linear range and data is normalized to unit loadings (1 lb. axial force, 1 lb. tip bending load, 1 in-lb. tip torque).

### Cross-Ply Results

The first set of validation cases is the bending and torsion of uncoupled cross-ply beams. Results of these tests are shown in Figures 5a-5c. Correlation between analytical solution, finite element solution and experimental data is excellent for all cross-ply cases.

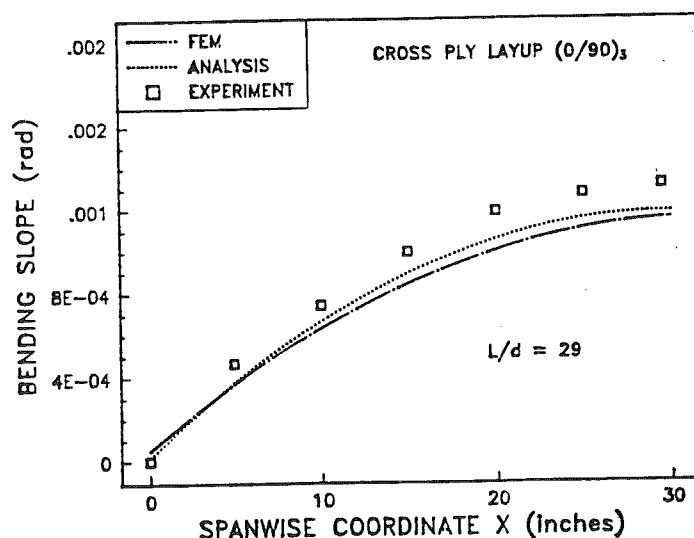


Figure 5a. Bending Slope Under Unit Tip Bending Load of Cross-Ply Layup Beam (L/d = 29)

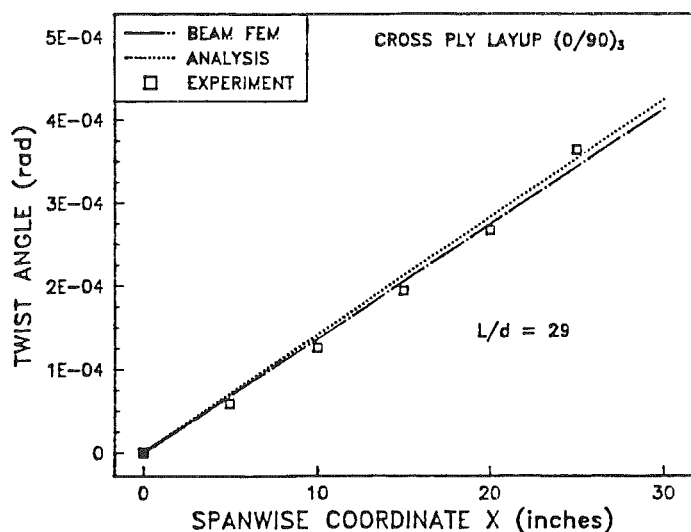


Figure 5b. Twist Under Unit Tip Torque of Cross-Ply Layup Beam ( $L/d = 29$ )

results of the refined beam finite element and the 3-D solid element are nearly identical.

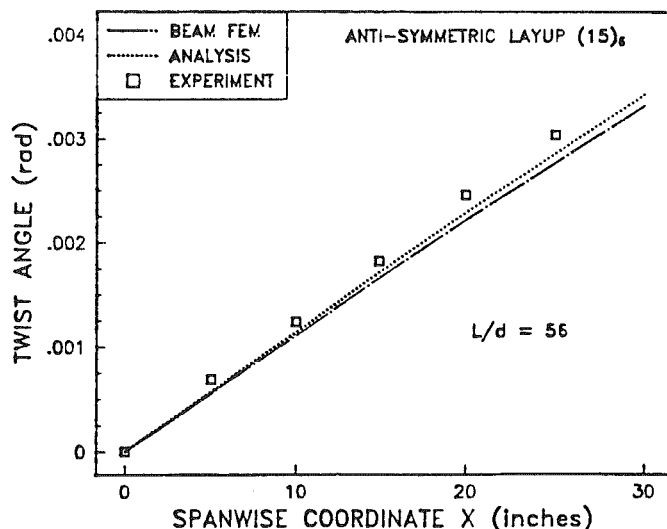


Figure 6a. Twist Under Unit Tip Torque of Anti-Symmetric Layup Beam ( $((15)_6, L/d = 56)$ )

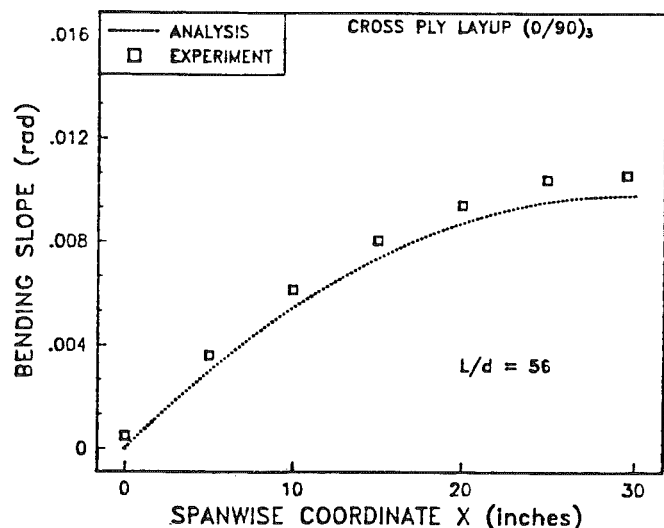


Figure 5c. Bending Slope Under Unit Tip Bending Load of Cross-Ply Layup Beam ( $L/d = 56$ )

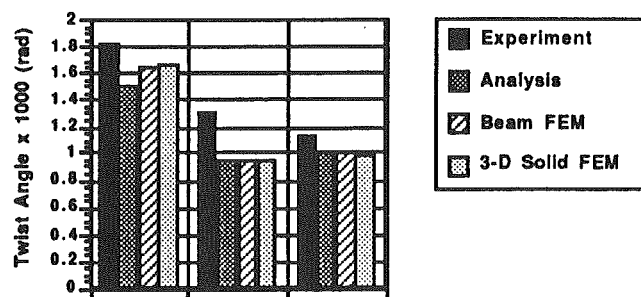


Figure 6b. Twist at  $x/R = 0.50$  Under Unit Tip Torque of Anti-Symmetric Layup Beams ( $L/d = 56$ )

### Anti-Symmetric Layup Results

The next set of test cases is the extension and torsion of anti-symmetric layup beams. Results of these tests are shown in Figures 6a-6c. This data is all linear as demonstrated in Figure 6a; therefore, only twist angles at mid-span are reported in Figures 6b-6c. Correlation between analytical solution and finite element solutions (refined beam element and 3-D solid element) is excellent. There is some margin of significant error between experimental data and both analytical and finite element solutions for twist of the  $(0/30)_3$  layup beam under tip torque. Note that

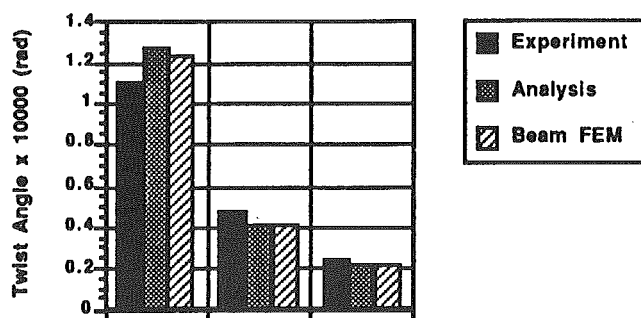


Figure 6c. Twist at  $x/R = 0.50$  Under Unit Tip Axial Force of Anti-Symmetric Layup Beams ( $L/d = 56$ )

## Symmetric Layup Results

Symmetric layup beams were tested under bending and torsional loading conditions. Figures 7a-7f show the spanwise distribution of bending slope and twist angle for symmetric layup beams subjected to a tip bending load. Correlation is satisfactory except for the twist angle of the beam with  $(45)_6$  top and bottom and  $(45/-45)_3$  sides. Results of torsional loading tests are shown in Figures 8a-8e. This data is also linear as demonstrated in Figure 8a; therefore, only mid-span twists and bending slopes are presented in Figures 8b-8e. Correlation is once again satisfactory except for the beams with  $(45)_6$  top and bottom and  $(45/-45)_3$  sides.

The analysis performed very well over almost all of the validation cases which were conducted. The only significant discrepancies were for beams with  $(45)_6$  top and bottom and  $(45/-45)_3$  sides. It is suspected that a more refined model of warping, and/or a more refined treatment of the transverse in-plane elastic behavior may alleviate this problem.

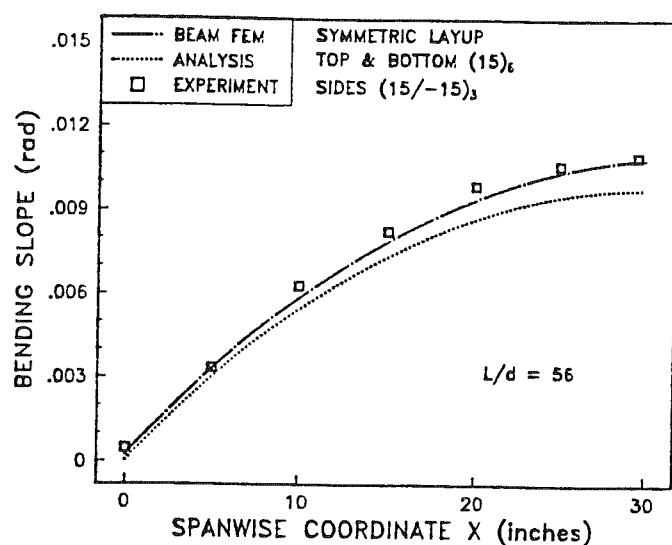


Figure 7a. Bending Slope Under Unit Tip Bending Load of Symmetric Layup Beam (Top & Bottom  $(15)_6$ , Sides  $(15/-15)_3$ ,  $L/d = 56$ )

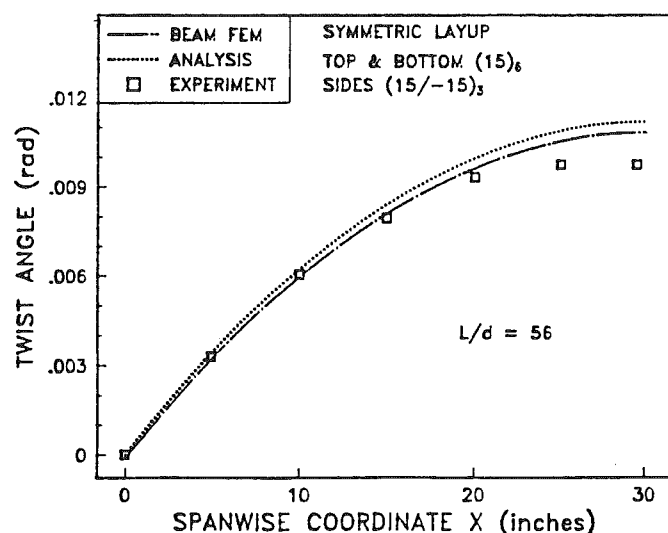


Figure 7b. Twist Under Unit Tip Bending Load of Symmetric Layup Beam (Top & Bottom  $(15)_6$ , Sides  $(15/-15)_3$ ,  $L/d = 56$ )

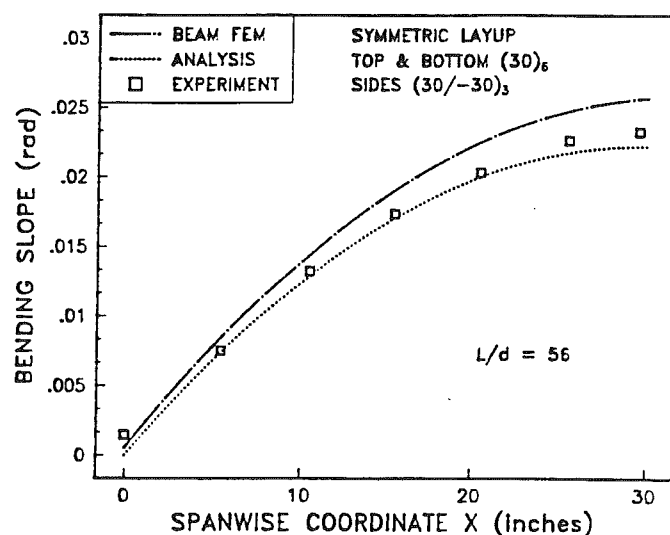


Figure 7c. Bending Slope Under Unit Tip Bending Load of Symmetric Layup Beam (Top & Bottom  $(30)_6$ , Sides  $(30/-30)_3$ ,  $L/d = 56$ )

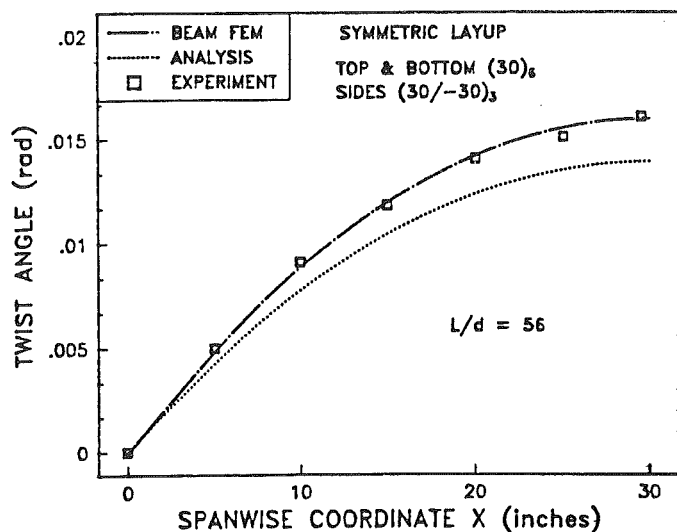


Figure 7d. Twist Under Unit Tip Bending Load of Symmetric Layup Beam (Top & Bottom (30)<sub>6</sub>, Sides (30/-30)<sub>3</sub>, L/d = 56)

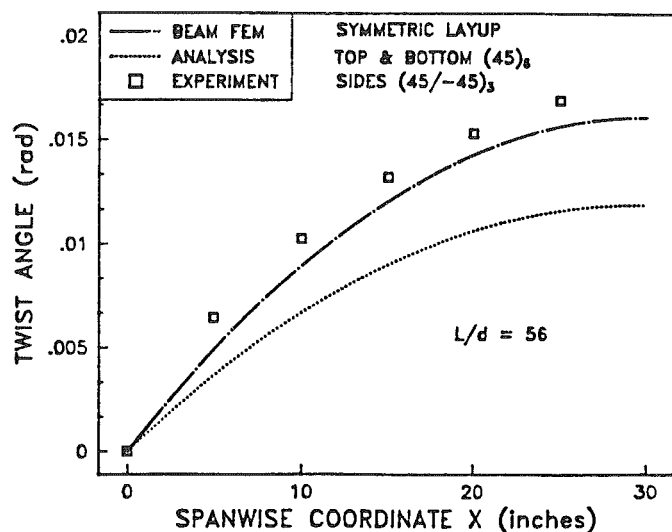


Figure 7f. Twist Under Unit Tip Bending Load of Symmetric Layup Beam (Top & Bottom (45)<sub>6</sub>, Sides (45/-45)<sub>3</sub>, L/d = 56)

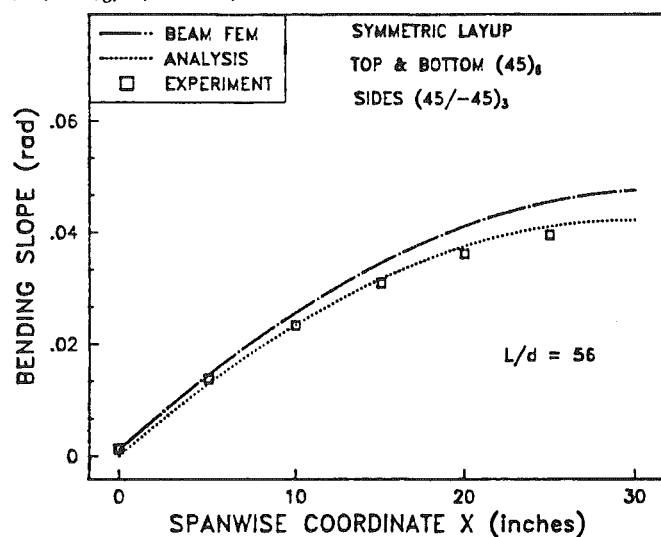


Figure 7e. Bending Slope Under Unit Tip Bending Load of Symmetric Layup Beam (Top & Bottom (45)<sub>6</sub>, Sides (45/-45)<sub>3</sub>, L/d = 56)

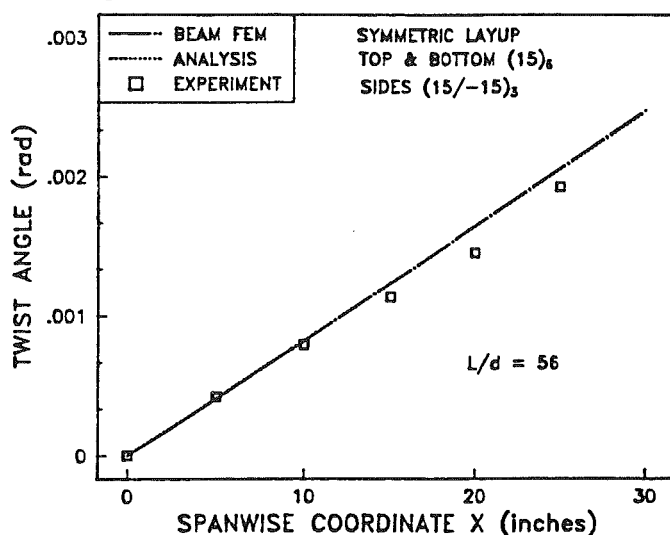


Figure 8a. Twist Under Unit Tip Torque of Symmetric Layup Beam (Top & Bottom (15)<sub>6</sub>, Sides (15/-15)<sub>3</sub>, L/d = 56)

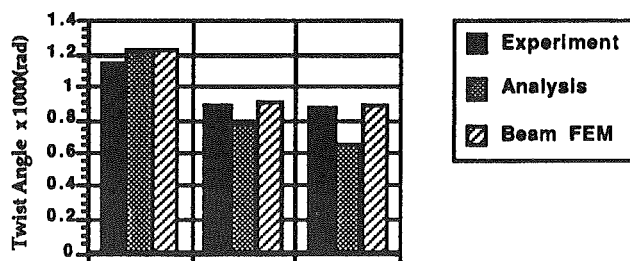


Figure 8b. Twist at  $x/R = 0.50$  Under Unit Tip Torque of Symmetric Layup Beams (L/d = 56)

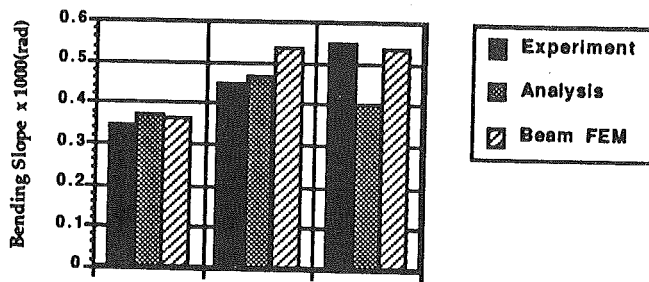


Figure 8c. Bending Slope at  $x/R = 0.50$  Under Unit Tip Torque of Symmetric Layup Beams ( $L/d = 56$ )

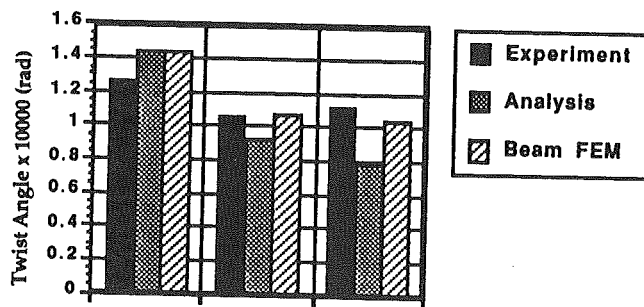


Figure 8d. Twist at  $x/R = 0.50$  Under Unit Tip Torque of Symmetric Layup Beams ( $L/d = 29$ )

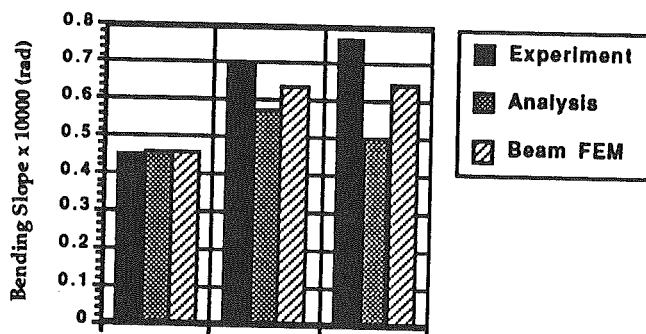


Figure 8e. Bending Slope at  $x/R = 0.50$  Under Unit Tip Torque of Symmetric Layup Beams ( $L/d = 29$ )

#### IV. Investigations of Non-classical Effects

##### *Torsion-Related Out-of-Plane Warping*

For beams composed of isotropic materials, rigorous elasticity solutions verify that the torsional stiffness

is indeed influenced by the torsion-related warping of the cross-section [38,42-44].

In the present analysis, the effects of torsion-related out-of-plane warping can be identified by examining the effective cross-sectional stiffnesses. For tailored composite box-beams, torsion-related warping can also influence coupling stiffnesses which are linked to the torsional deformation of the beam. This is indicated by the presence of terms involving  $\beta$  in the torsional stiffness, and coupling stiffnesses involving torsion. For example, consider the torsional stiffness,  $K_{44}$ , and bending-torsion coupling stiffnesses  $K_{45}$ , and  $K_{46}$

$$K_{44} = (1 + \beta)^2 \int_h \bar{Q}_{66} \zeta^2 dA + (1 - \beta)^2 \int_v \bar{Q}_{66} \eta^2 dA \quad [A9]$$

$$+ d_0 \left[ (1 - \beta) \int_v \bar{Q}_{26} \eta dA - (1 + \beta) \int_h \bar{Q}_{26} \zeta dA \right]$$

$$+ d_1 (1 - \beta) \int_v \bar{Q}_{26} \eta^2 dA - d_2 (1 + \beta) \int_h \bar{Q}_{26} \zeta^2 dA$$

$$K_{45} = (1 + \beta) \int_h \bar{Q}_{16} \zeta^2 dA + d_2 \int_{h,v} \bar{Q}_{12} \zeta^2 dA \quad [A10]$$

$$K_{46} = - (1 - \beta) \int_v \bar{Q}_{16} \eta^2 dA + d_1 \int_{h,v} \bar{Q}_{12} \eta^2 dA \quad [A11]$$

For box-beams designed with isotropic materials, the warping is typically a function of geometry only. This is not necessarily true for composite box-beams. The use of composite materials to tailor box-beam structures opens the possibility of designed variations in stiffness around the beam cross-section. To design a structure with different amounts of bending-torsion couplings about each bending axis (spanwise bending or chordwise bending), the top and bottom of the box-beam must consist of different composite laminates. By examining the warping parameter  $\alpha$ , the effects of variations in stiffness around the cross-section on the warping become apparent.

$$\alpha = \left( \frac{c}{d} \right) \left( \frac{t_v}{t_h} \right) \left( \frac{G_v}{G_h} \right) \quad [8]$$

If the laminate varies around the cross-section, the effective modulus will change and  $G_v$  will differ from

$G_h$ . For example, this is the case for the symmetric layup box-beams used in the validation study. The top and bottom of these beams are  $(\theta)_6$ , and the sides are  $(\theta/-\theta)_3$ . Contribution to beam elastic couplings are strong in the top and bottom walls and weak in the side walls.

The influence of warping on the elastic behavior of the box-beam is isolated by examining load deflection results generated both with and without warping included in the formulation. Results without warping are achieved by setting  $\beta=0$ . Considering the initial kinematic assumptions, this is equivalent to removing the warping component from the axial deformation  $U$ . Effects of neglecting the variation in stiffness around the cross-section are demonstrated by setting  $G_v = G_h$  and again examining the results. This restrictive assumption is very common in analyses of thin-walled metallic beams.

The effects of warping are demonstrated in Figures 9a-c. Tip twist of anti-symmetric layup box-beams, with  $(\theta)_6$  walls, under unit tip torque are shown in Figure 9a. As the effective torsional stiffness increases ( $\theta$  approaches 45 degrees), the effects of warping becomes more severe. Figure 9b illustrates the effects of warping on the tip twist of symmetric layup beams with top and bottom  $(\theta)_6$ , and sides  $(\theta/-\theta)_3$  subjected to unit tip torque. Once again the effects of warping are most severe at the point of maximum effective torsional stiffness. The effects of warping on the bending-torsion coupling behavior of these symmetric layup beams are the most dramatic of the cases presently investigated. Figure 9c shows the tip twist under unit tip bending load of symmetric layup beams with top and bottom  $(\theta)_6$  and sides  $(\theta/-\theta)_3$ . Warping causes an increase (over results without warping included) of over 200% in this coupled deformation. Also note the impact of ignoring the variation in stiffness around the cross-section. This effect alone causes nearly a 100% increase in coupled deformation. As indicated by experimental correlation shown in Figure 9c, the new warping approach used in the present analysis effectively captures the drastically increased warping effect due to variations in stiffness around the cross-section.

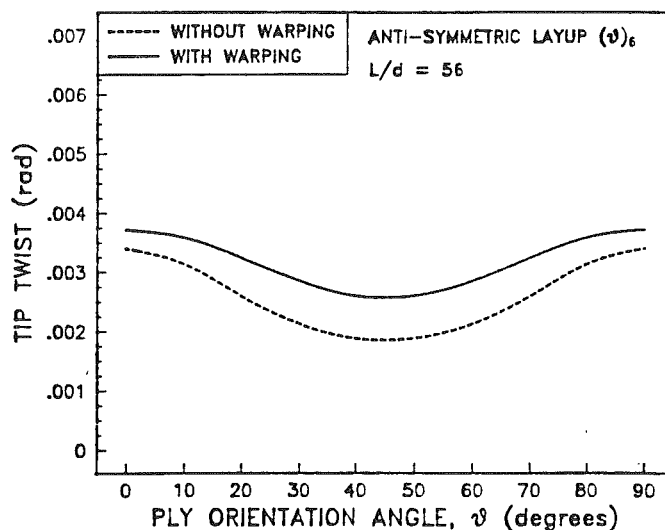


Figure 9a. Tip Twist Under Unit Tip Torque of Anti-Symmetric Layup Beams ( $(\theta)_6$ ,  $L/d = 56$ )

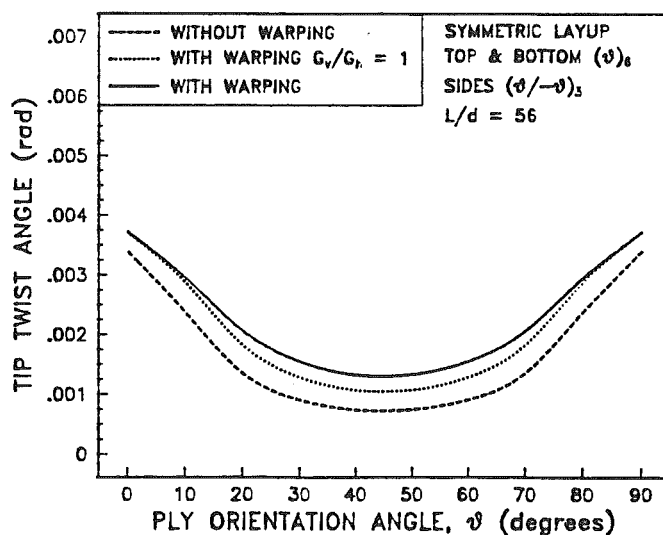


Figure 9b. Tip Twist Under Unit Tip Torque of Symmetric Layup Beams (Top & Bottom  $(\theta)_6$ , Sides  $(\theta/-\theta)_3$ ,  $L/d = 56$ )

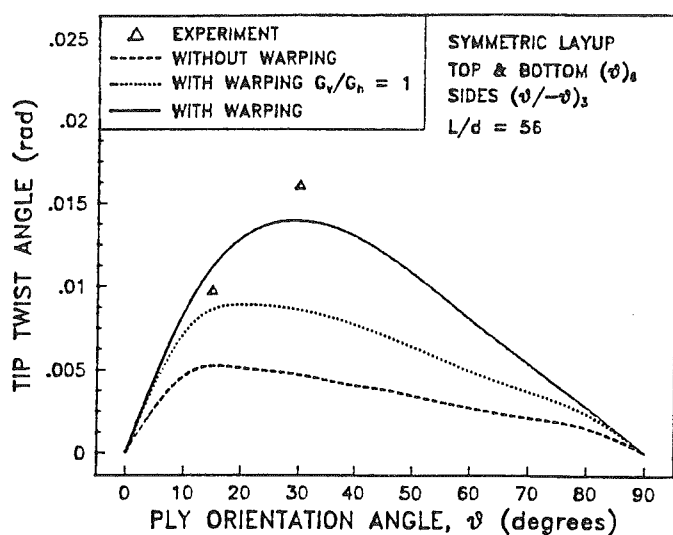


Figure 9c. Tip Twist Under Unit Tip Bending Load of Symmetric Layup Beams (Top & Bottom  $(\theta)_6$ , Sides  $(\theta/-\theta)_3$ ,  $L/d = 56$ )

The focus of this discussion has been on the analytic treatment of torsion-related out-of-plane warping. When boundary conditions are such that this deformation is restricted, localized phenomenon called warping restraint effects can occur. This effect can be more pronounced for composite designs than for metallic designs. Research has indicated that warping restraint effects are most important for relatively short beams or plate structures such as those used in wings of a fighter aircraft [45,46]. Warping restraint effects can also be dominant in torsion problems of open sections. The closed section box-beams analyzed in the present study are very slender and the effects of localized warping restraint on the beam deflections are assumed to be negligible.

#### Transverse Shear

Typically, transverse shear deformation of beam cross-sections is not very important in the analysis of slender beams. The existence of elastic couplings can change this notion dramatically. The work of Rehfield, Atilgan, and Hodges [22] deserves credit for shedding light on this interesting behavior.

By including transverse shear deformation in the kinematics of the analysis, it is possible to identify elastic couplings between transverse shear and bending, and between transverse shear and extension. These couplings arise due to the coupling between

extension and in-plane shear which can exist in the anisotropic plies in the beam walls. The physical origins of these unique coupling mechanisms are illustrated in Figure 10.

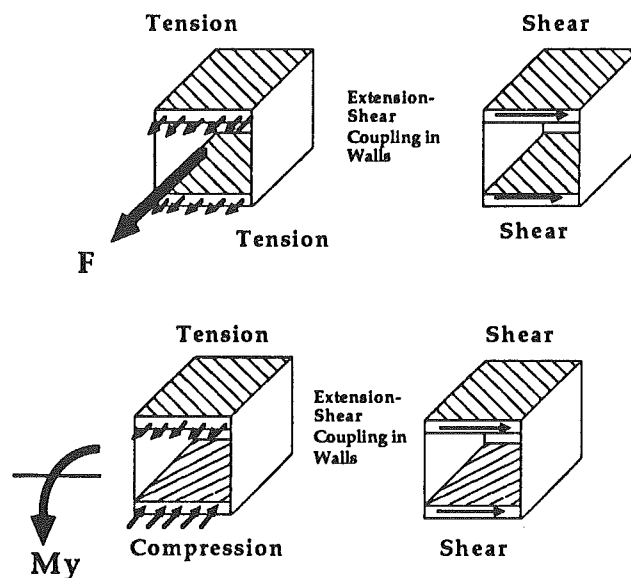


Figure 10. Shear Coupling Mechanisms

While the actual shearing component of the deformation is still relatively small for slender beams, the presence of shear couplings can effectively increase beam compliance in either bending or extension. This concept can be clarified by considering the governing differential equations of a box beam with anti-symmetric layup. This configuration displays extension-torsion coupling and bending-shear couplings. Beam compliance can be evaluated by examining the inverse of the beam stiffness matrix  $K$ . The details of the algebraic manipulations are presented in Appendix C. Upon examination of the beam compliances, it is established that bending-shear coupling can increase the direct bending compliance of the beam. In a similar manner, extension-shear couplings can increase the axial compliance of symmetric layup box-beams. Details of the algebraic manipulations are again presented in Appendix C.

Results illustrating the quantitative effects of bending-shear couplings on the effective bending stiffness of anti-symmetric layup box-beams are shown in Figures 11a-e. The reduction in effective bending stiffness (inversely related to increase in

bending compliance) for both  $(\theta)_6$  and  $(0/\theta)_3$  anti-symmetric layups is shown in Figure 11a. The results shown in Figure 11a are for beams constructed from unidirectional plies, similar analytical results are shown in Figure 11b for beams constructed from cloth plies. Material properties for unidirectional and cloth ply materials are provided in Table 3. Both figures demonstrate that the reduction in effective bending stiffness due to bending shear couplings varies significantly with ply orientation angle. Reductions in effective stiffness can become very significant for both unidirectional and cloth ply designs. For both types of ply, reduction in stiffness is more severe for the  $(\theta)_6$  design than for the  $(0/\theta)_3$  design. It is important to note that elastic couplings are also generally stronger in the  $(\theta)_6$  design.

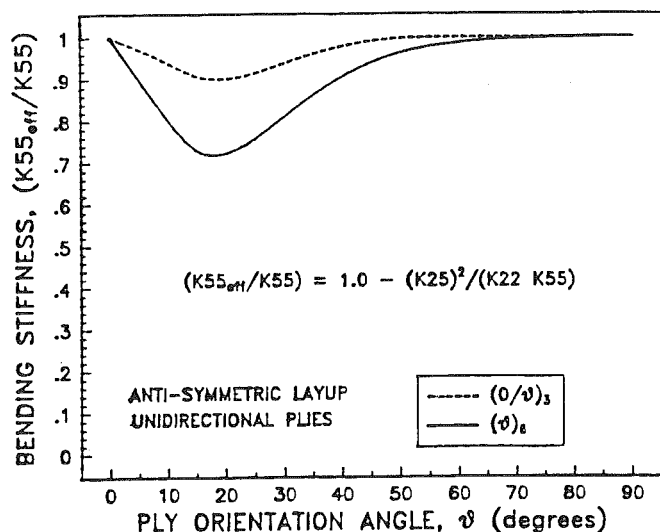


Figure 11a. Reduction in Effective Bending Stiffness Due to Shear Couplings of Anti-Symmetric Layup Beams (Unidirectional Plies,  $(\theta)_6$ , and  $(0/\theta)_3$ ,  $L/d = 56$ )

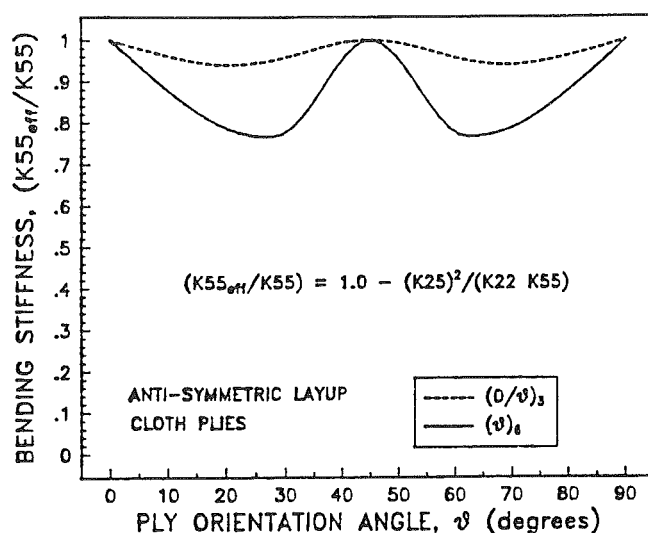


Figure 11b. Reduction in Effective Bending Stiffness Due to Shear Couplings of Anti-Symmetric Layup Beams (Cloth Plies,  $(\theta)_6$ , and  $(0/\theta)_3$ ,  $L/d = 56$ )

the analytical results are presented. The version without transverse shear has all direct shear and shear-related coupling terms set to zero. Correlation between analysis and experiment is excellent for all three composite designs. These results clearly demonstrate how the particular composite design can influence the degree of compliance increase due to bending-shear couplings.

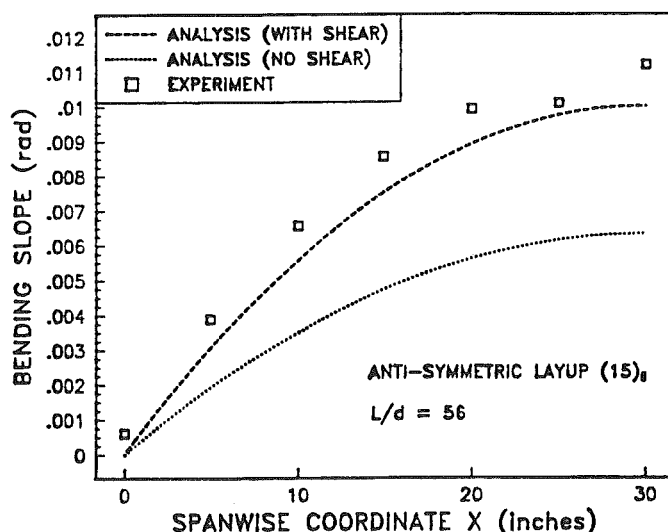


Figure 11c. Bending Slope Under Unit Tip Bending Load of Anti-Symmetric Layup Beam  $((15)_6$ ,  $L/d = 56$ )

Experimental verification of the quantitative effects of bending-shear couplings are presented in Figures 11c-e. These figures show both experimentally measured and analytically predicted spanwise bending slopes of  $(15)_6$ ,  $(0/30)_3$ , and  $(0/45)_3$  anti-symmetric layup box-beams. These beams are the same anti-symmetric layup beams used in the earlier validation and evaluation studies. Two versions of



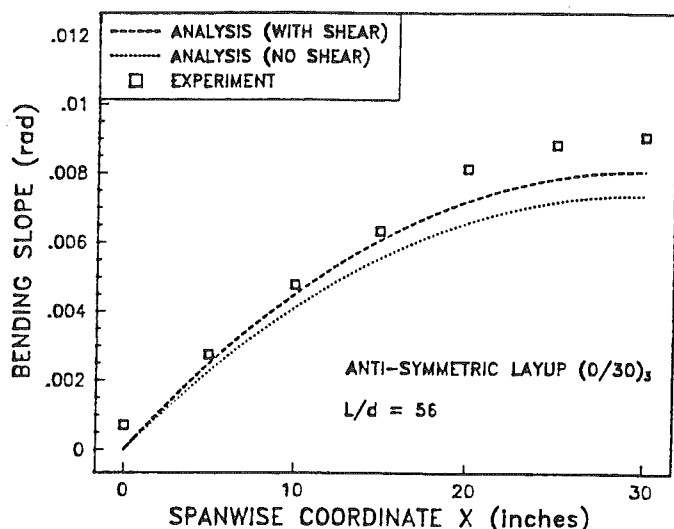


Figure 11d. Bending Slope Under Unit Tip Bending Load of Anti-Symmetric Layup Beam ((0/30)<sub>3</sub>, L/d = 56)

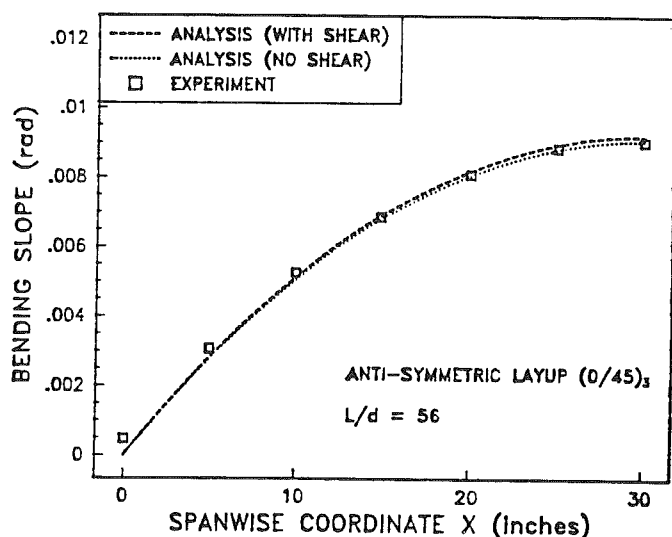


Figure 11e. Bending Slope Under Unit Tip Bending Load of Anti-Symmetric Layup Beam ((0/45)<sub>3</sub>, L/d = 56)

### Two-Dimensional In-Plane Elastic Behavior

Adequate treatment of the transverse in-plane stresses and strains,  $\sigma_{yy}$  and  $\epsilon_{yy}$ , can be important in composite box-beam analysis. Elastic properties within the composite plies vary dramatically with

ply orientation angle. For some composite designs, Poisson's effect can become very significant, causing the plies to behave in a highly two-dimensional elastic manner. Since the walls of the composite box-beam are built up from laminated plies, mismatch of Poisson's effect between plies within a wall can cause in-plane stresses and strains to exist even if there are no in-plane applied loads. This behavior is similar in nature to the thermally induced strains and stresses which result from mismatch in ply thermal expansion coefficients.

For long slender structures such as helicopter rotor blades, beam theory is more desirable than plate theory from both computational and design viewpoints. Beam theory is essentially one-dimensional; therefore, accurately capturing the two-dimensional behavior of composite plies with a beam analysis can be challenging.

Three methods for accounting for in-plane elastic behavior are investigated. Recall that subscript  $y$  pertains to  $\eta$  in horizontal walls and  $\zeta$  in vertical walls.

#### Method 1

The first method is closest to standard beam theory. Based only on initial kinematic assumptions about the deformations of the beam

$$\epsilon_{yy} = 0 \quad [23a]$$

and

$\sigma_{yy}$  has no effect on net cross-section forces and moments.

These conditions result in simplification of the ply elastic constitutive relations to

$$\begin{Bmatrix} \sigma_{xx} \\ \sigma_{xy} \end{Bmatrix} = \begin{bmatrix} \bar{Q}_{11} & \bar{Q}_{16} \\ \bar{Q}_{16} & \bar{Q}_{66} \end{bmatrix} \begin{Bmatrix} \epsilon_{xx} \\ \epsilon_{xy} \end{Bmatrix} \quad [23b]$$

#### Method 2

The second method begins to address the transverse in-plane behavior. In this method

$$\sigma_{yy} = 0 \quad [24a]$$

and  $\epsilon_{yy}$  is removed from the constitutive relation by substitution. This results in a modified constitutive relation

$$\begin{Bmatrix} \sigma_{xx} \\ \sigma_{xy} \end{Bmatrix} = \begin{bmatrix} \bar{Q}'_{11} & \bar{Q}'_{16} \\ \bar{Q}'_{16} & \bar{Q}'_{66} \end{bmatrix} \begin{Bmatrix} \epsilon_{xx} \\ \epsilon_{xy} \end{Bmatrix} \quad [24b]$$

with modified stiffness matrix  $Q'$  defined as

$$\begin{bmatrix} \bar{Q}'_{11} & \bar{Q}'_{16} \\ \bar{Q}'_{16} & \bar{Q}'_{66} \end{bmatrix} = \begin{bmatrix} \left( \bar{Q}_{11} - \frac{(\bar{Q}_{12})^2}{\bar{Q}_{22}} \right) & \left( \bar{Q}_{16} - \frac{\bar{Q}_{12}\bar{Q}_{26}}{\bar{Q}_{22}} \right) \\ \left( \bar{Q}_{16} - \frac{\bar{Q}_{12}\bar{Q}_{26}}{\bar{Q}_{22}} \right) & \left( \bar{Q}_{66} - \frac{(\bar{Q}_{26})^2}{\bar{Q}_{22}} \right) \end{bmatrix} \quad [25]$$

### Method 3

The third method treats the transverse in-plane behavior in a more refined manner. Conditions on the in-plane stresses and strains are imposed such that there are no in-plane forces or moments. This method has been discussed in detail during the description of the analysis formulation.

The difference between Method 1, Method 2 and Method 3 can be clarified by considering one of the resulting stiffness coefficients. For example, the axial stiffness of the box-beam as derived from Method 1, is given by

$$K_{11} = \int \int_{h,v} \bar{Q}_{11} dA \quad [26]$$

Axial stiffness derived using Method 2 is given by

$$K_{11} = \int \int_{h,v} \left[ \bar{Q}_{11} - \frac{\bar{Q}_{12}^2}{\bar{Q}_{22}} \right] dA \quad [27]$$

Axial stiffness derived using Method 3 is given by

$$K_{11} = \int \int_{h,v} \bar{Q}_{11} dA - \frac{\int \int_{h,v} \bar{Q}_{12} dA \int \int_{h,v} \bar{Q}_{12} dA}{\int \int_{h,v} \bar{Q}_{22} dA} \quad [28]$$

Note the differences in the manner in which two-dimensional in-plane elastic behavior appears in the different expressions for axial stiffness.

The quantitative differences between the three methods previously described are illustrated in Figures 11a-b. In addition to analytical results,

experimental results from pertinent validation cases are shown in Figures 12a-b. Tip twist under unit tip torque of  $(0/\theta)_3$  anti-symmetric layup beams is shown in Figure 12a. Note that at ply orientation angles  $\theta < 20$  degrees, the differences between all three methods are quite small. As ply orientation angle increases, two-dimensional effects become more significant and the deviation between the three methods becomes large. The standard beam theory approach (Method 1,  $\epsilon_{yy} = 0$ ) is clearly inadequate for these cases. Method 2,  $\sigma_{yy} = 0$ , represents an improvement over standard beam theory, however, the refined approach used in the present analysis (Method 3) is the most effective.

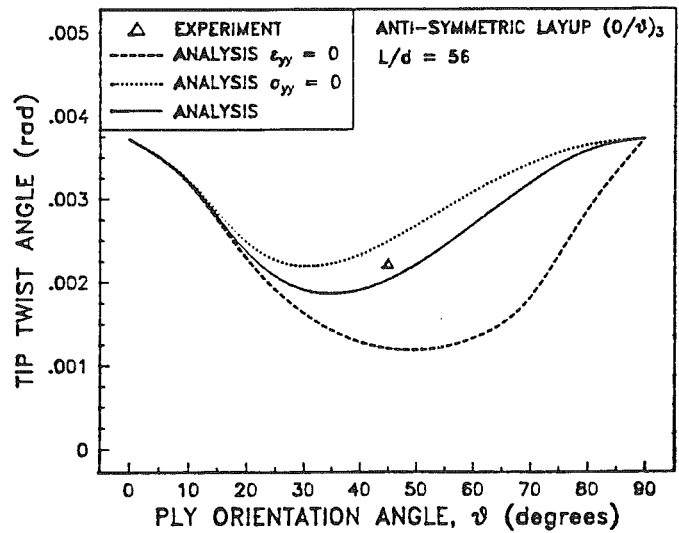


Figure 12a. Tip Twist Under Unit Tip Torque of Anti-Symmetric Layup Beams  $((0/\theta)_3, L/d = 56)$

Tip twist under unit axial force of  $(0/\theta)_3$  anti-symmetric layup beams is shown in Figure 12b. This is a coupling effect. Once again the standard beam theory approach is inadequate. In this, deviation between Method 2 and Method 3 is very small.

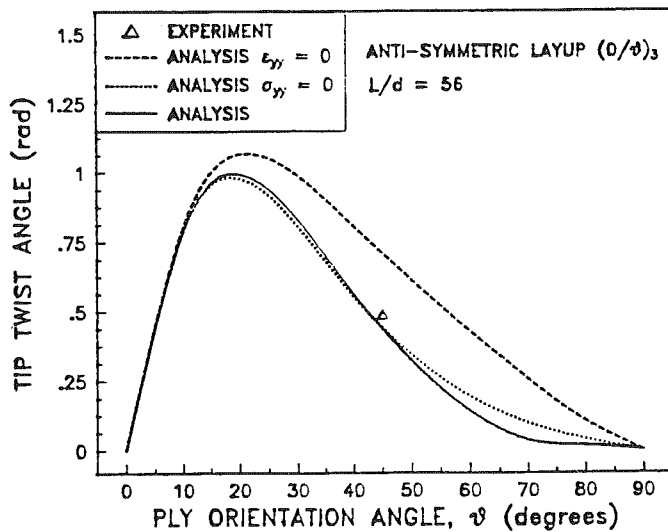


Figure 12b. Tip Twist Under Unit Tip Axial Force of Anti-Symmetric Layup Beams  $((0/\theta)_3, L/d = 56)$

## V. Conclusions

Based on the investigations carried out during this research, the following conclusions are drawn:

- 1) Correlation between analysis, experiment, and detailed finite element solutions is quite good for all cross-ply and anti-symmetric layup validation test cases.
- 2) The only significant discrepancies between analysis, experiment, and detailed finite element solutions are at high ply orientation angles ( $\theta > 30$  degrees) for symmetric layup beams with variations in stiffness around the cross-section.
- 3) Torsion-related out-of-plane warping can significantly effect the torsional and torsion-related coupling stiffnesses of tailored composite box-beams. These effects can be dramatic in highly coupled symmetric layup beams, causing up to 200% increase in coupled deformations. Variations in stiffness around the beam cross-section can also significantly effect the warping and torsional behavior of the

beam. Not accounting for (in the warping shape) variations in stiffness can cause 100% error in highly coupled symmetric layup beams.

4) Transverse shear couplings can dramatically alter the elastic response of tailored composite box-beams. For example, bending-shear couplings can reduce the effective bending stiffness of highly coupled anti-symmetric layup beams by more than 30%.

5) Capturing two-dimensional elastic behavior of the composite plies is essential for accurate analysis of tailored composite box-beams. Load deflection results for anti-symmetric beams can be altered by 30-100% by not accounting for this elastic behavior.

6) This direct analytical method can be easily implemented into comprehensive dynamic analyses for composite rotor systems. The analytical results can efficiently provide elastic stiffness and coupling properties which are crucial to composite rotor dynamics problems.

## Acknowledgements

The authors would like to thank Dr. Ramesh Chandra for providing the wide array of high quality experimental results and sharing his expertise in many beneficial technical discussions. Dr. Alan Stemple and Dr. Y. Kim also deserve thanks for their help in making the finite element programs available. This research work was jointly supported by the Army Aerostructures Directorate, Grant No. NAG-1-853; Technical Monitor Mr. Mark W. Nixon, and the Army Research Office, Contract No. DAAL-03-88-C002; Technical Monitors Dr. Robert Singleton and Dr. Tom Doligalski.

## References

1. Weisshaar, T., "Aeroelastic Tailoring - Creative Uses of Unusual Materials", AIAA Paper No. 87-0976-CP, 1987.
2. Hong, Chang-Ho and Chopra, I., "Aeroelastic Stability Analysis of a Composite Blade," *Proceedings of the 40th Annual Forum of the American Helicopter Society*, 1984.

3. Hong, Chang-Ho and Chopra, I., "Aeroelastic Stability Analysis of a Composite Bearingless Rotor Blade," *Presented at the International Conference on Rotorcraft Basic Research*, February, 1985.
4. Panda, B. and Chopra, I., "Dynamics of Composite Rotor Blades in Forward Flight," *Vertica*, Vol. 11, (1/2), 1987.
5. Nixon, M. W., "Extension-Twist Coupling of Composite Circular Tubes With Application to Tilt Rotor Blade Design," *Proceedings of the AIAA/ASME/ASCE/AHS 28th Structures, Structural Dynamics and Materials Conference*, April 1987.
6. Worndle, R., "Calculation of The Cross Section Properties and The Shear Stress of Composite Rotor Blades," *Presented at Seventh European Rotorcraft and Powered Lift Aircraft Forum*, September 1981.
7. Giavotto, V., Borri, M., et al., "Anisotropic Beam Theory and Applications," *Computers & Structures*, Vol. 16, (1-4), 1983.
8. Borri, M. and Merlini, T., "A Large Displacement Formulation For Anisotropic Beam Analysis," *Meccanica*, Vol. 21, 1986.
9. Bauchau, O. A. and Hong, Chang-Hee, "Finite Element Approach to Rotor Blade Modeling," *Presented at the Dynamics and Aeroelastic Stability Modelling of Rotor Systems Technical Workshop*, December 1985.
10. Bauchau, O. A. and Hong, C. H., "Large Displacement Analysis of Naturally Curved and Twisted Composite Beams," *AIAA Journal*, Vol. 25, (10), October 1987.
11. Bauchau, O. A. and Hong, C. H., "Nonlinear Composite Beam Theory," *Journal of Applied Mechanics*, Vol. 55, March 1988.
12. Stemple, A. D. and Lee, S. W., "Finite Element Model For Composite Beams With Arbitrary Cross Sectional Warping," *AIAA Journal*, Vol. 26, (12), December 1988.
13. Stemple, A. D. and Lee, S. W., "A Finite Element Model For Composite Beams Undergoing Large Deflection With Arbitrary Cross Sectional Warping," *Presented at the Second International Conference on Basic Rotorcraft Research*, February, 1988.
14. Stemple, A. D. and Lee, S. W., "Large Deflection Static and Dynamic Finite Element Analyses of Composite Beams with Arbitrary Cross Sectional Warping," *Proceeding of the 28th AIAA/ASME/ASCE/AHS/ASC Structures, Structural Dynamics and Materials Conference*, 1989.
15. Kosmatka, J. B. and Friedmann, P. P., "Structural Dynamic Modeling of Advanced Composite Propellers By the Finite Element Method," *Proceedings of the 28th AIAA/ASME/ASCE/AHS Structures, Structural Dynamics and Materials Conference*, 1989.
16. Kosmatka, J. B., "A Refined Beam Theory For Advanced Composite Rotor Blade Analysis," *Proceedings of American Helicopter Society National Technical Specialists' Meeting on Advanced Rotorcraft Structures*, October 1988.
17. Kosmatka, J. B., "Extension, Bending and Torsion of Anisotropic Beams With Initial Twist," *Proceedings of the 30th AIAA/ASME/ASCE/AHS/ASC Structures, Structural Dynamics and Materials Conference*, 1989.
18. Nixon, M., "Analytical and Experimental Investigations Of Extension-Twist Coupled Structures", M.S. Thesis, NASA Langley/ George Washington University, 1989.
19. Reissner, E. and Tsai, W. T., "Pure Bending, Stretching, and Twisting of Anisotropic Cylindrical Shells," *Journal of Applied Mechanics*, March 1972.
20. Mansfield, E. H. and Sobey, A. J., "The Fibre Composite Helicopter Blade; Part 1: Stiffness Properties; Part 2: Prospects for Aeroelastic Tailoring," *Aeronautical Quarterly*, May 1979.
21. Rehfield, L. W., "Design Analysis Methodology for Composite Rotor Blades," *Presented at Seventh DoD/NASA Conference on Fibrous Composites in Structural Design*, June 1985.
22. Hodges, D. H., Nixon, M. W., and Rehfield, L. W., "Comparison of Composite Rotor Blade

Models: A Coupled Beam Analysis and an MSC NASTRAN Finite Element Model," NASA Technical Memorandum 89024, 1987.

23. Rehfield, L. W., Hodges, D. H., and Atilgan, A. R., "Some Considerations on the Non-Classical Behavior of Thin-Walled Composite Beams," *Proceedings of American Helicopter Society National Technical Specialists' Meeting on Advanced Rotorcraft Structures*, October 1988.
24. Bauchau, O. A., "A Beam Theory For Anisotropic Materials," *Journal of Applied Mechanics*, Vol. 52, June 1985.
25. Bicos, A. S., and Springer, G. S., "Design of a Composite Box-Beam," *Journal of Composite Materials*, Vol. 20, January 1986.
26. Libove, C., "Stresses and Rate of Twist in Single-Cell Thin-Walled Beams with Anisotropic Walls," *AIAA Journal*, Vol. 26, September 1988.
27. Chang, S. I., and Libove, C., Shear Flows, Strains, and Rate of Twist in Single-Cell Thin-Walled Beams with Anisotropic Walls: Simple Theory Compared With NASTRAN and Experiment," *Presented at The ASME Winter Annual Meeting*, 1988.
28. Klang, E. C., and Kuo, T. M., "Component Level Analysis of Composite Box-Beams," *Proceedings of the 30th AIAA/ASME/ ASCE/AHS/ASC Structures, Structural Dynamics and Materials Conference*, 1989.
29. Rand, O., "Theoretical modelling of Composite Rotating Beams," TAE Report No. 633 Technion - Israel Institute of Technology, Haifa, Israel, October 1988.
30. Rand, O., "Periodic Response of Thin-Walled Composite Blades," *Proceedings of the 30th AIAA/ ASME/ ASCE/AHS/ASC Structures, Structural Dynamics and Materials Conference*, 1989.
31. Minguet, P., and Dugundji, J., "Experiments and Analysis for Structurally Coupled Composite Blades Under Large Deflections Part 1 Statics, Part 2 Dynamics," *Proceedings of the 30th AIAA/ASME/ ASCE/AHS/ASC Structures, Structural Dynamics and Materials Conference*, 1989.
32. Minguet, P., "Static and Dynamic Behavior of Composite Helicopter Rotor Blades Under Large Deflection," PhD. Thesis, Massachusetts Institute of Technology, 1989.
33. Murray, N. W., "Chapters 1-3," *Introduction to the Theory of Thin-Walled Structures*, Clarendon Press, Oxford, 1986.
34. Gjelsvik, A., "Chapters 1-5," *The Theory of Thin Walled Bars*, John Wiley & Sons, New York, 1981.
35. Kollbrunner, C. F., and Basler, K., Translated from German by Glauser, E. C., "Chapters 1-3," *Torsion in Structures An Engineering Approach*, Springer-Verlag, New York, 1969.
36. Megson, T. H. G., "Chapter 5 Torsion of Closed and Open Sections," *Linear Analysis of Thin-Walled Elastic Structures*, John Wiley & Sons, New York, 1974.
37. Jones, R. M., "Chapters 2 -4," *Mechanics of Composite Materials*, Hemisphere Publishing Corporation, New York, 1975.
38. Brunelle, E. J., "Dynamical Torsion Theory of Rods Deduced From the Equations of Linear Elasticity," *AIAA Journal*, Vol. 10, (4), April 1971.
39. Chandra, R., Ngo, H., and Chopra, I., "Experimental Study of Thin-Walled Composite Beams," *Presented at American Helicopter Society National Technical Specialists' Meeting on Advanced Rotorcraft Structures*, October 1988.
40. Chandra, R., Stemple, A. D., and Chopra, I., "Thin-Walled Composite Beams Under Bending Torsional, and Extensional Loads," Accepted for Publication in *Journal of Aircraft*.
41. Kim, Y. H., and Lee, S. W., "A Solid Element Formulation For Large Deflection Analysis of Composite Shell Structures," *Computers & Structures*, Vol. 30, (1/2), 1988.
42. Sokolnikoff, I. S., "Chapter 4 Extension, Torsion and Flexure of Beams," *Mathematical Theory of Elasticity*, McGraw-Hill Book Company Inc., New York, 1956.

43. Timoshenko, S. P., and Goodier, J. N., "Chapter 10 Torsion," *Theory of Elasticity*, Third Edition, McGraw-Hill Book Company Inc., New York, 1970.
44. Lekhnitskii, S. G., English Translation by Mir Publishers, "Chapter 6 Generalized Torsion and Torsion of Bars," *Theory of Elasticity of an Anisotropic Body*, Mir Publishers, Moscow, 1981.
45. Oyibo, G. A., and Berman, J. H., "Influence of Warp on Composite Aeroelastic Theories," AIAA Paper No. 85-0710, 1985.
46. Librescu, L., and Khdeir, A. A., "Aeroelastic Divergence of Swept-Forward Composite Wings Including Warping Restraint Effect," *AIAA Journal*, Vol. 26, (11), November 1988.

## Appendix A . Elements of Box-Beam Stiffness Matrix K

The following non-zero beam stiffness matrix terms are defined for use in cross-ply, anti-symmetric, or symmetric layup composite box-beams. If the beam cross-section does not display any symmetry, all 21 coefficients may be non-zero.

- $K_{11}$  = axial stiffness  
 $K_{12}$  = extension-chordwise shear coupling stiffness  
 $K_{13}$  = extension-spanwise shear coupling stiffness  
 $K_{14}$  = extension-torsion coupling stiffness  
 $K_{22}$  = chordwise shear stiffness  
 $K_{25}$  = spanwise bending-chordwise shear coupling stiffness  
 $K_{33}$  = spanwise shear stiffness  
 $K_{36}$  = chordwise bending-spanwise shear coupling stiffness  
 $K_{44}$  = torsional stiffness  
 $K_{45}$  = spanwise bending-torsion coupling stiffness  
 $K_{46}$  = chordwise bending-torsion coupling stiffness  
 $K_{55}$  = spanwise bending stiffness  
 $K_{66}$  = chordwise bending stiffness

$$K_{11} = \int \int_{h,v} \bar{Q}_{11} dA + a_0 \int \int_{h,v} \bar{Q}_{12} dA \quad [A1]$$

$$K_{12} = \int \int_h \bar{Q}_{16} dA + f_0 \int \int_h \bar{Q}_{12} dA \quad [A2]$$

$$K_{13} = \int \int_v \bar{Q}_{16} dA + g_0 \int \int_v \bar{Q}_{12} dA \quad [A3]$$

$$K_{14} = -(1 + \beta) \int \int_h \bar{Q}_{16} \zeta dA + (1 - \beta) \int \int_v \bar{Q}_{16} \eta dA + d_0 \int \int_{h,v} \bar{Q}_{12} dA \quad [A4]$$

$$K_{22} = \int \int_h \bar{Q}_{66} dA + f_0 \int \int_h \bar{Q}_{26} dA \quad [A5]$$

$$K_{25} = \int \int_h \bar{Q}_{16} \zeta dA + f_2 \int \int_h \bar{Q}_{12} dA \quad [A6]$$

$$K_{33} = \int \int_v \bar{Q}_{66} dA + g_0 \int \int_v \bar{Q}_{26} dA \quad [A7]$$

$$K_{36} = \int \int_v \bar{Q}_{16} \eta dA + g_1 \int \int_v \bar{Q}_{12} dA \quad [A8]$$

$$K_{44} = (1 + \beta)^2 \int \int_h \bar{Q}_{66} \zeta^2 dA + (1 - \beta)^2 \int \int_v \bar{Q}_{66} \eta^2 dA + d_0 \left[ (1 - \beta) \int \int_v \bar{Q}_{26} \eta dA - (1 + \beta) \int \int_h \bar{Q}_{26} \zeta dA \right] \quad [A9]$$

$$+ d_1 (1 - \beta) \int \int_v \bar{Q}_{26} \eta^2 dA - d_2 (1 + \beta) \int \int_h \bar{Q}_{26} \zeta^2 dA$$

$$K_{45} = (1 + \beta) \int \int_h \bar{Q}_{16} \zeta^2 dA - d_2 \int \int_{h,v} \bar{Q}_{12} \zeta^2 dA \quad [A10]$$

$$K_{46} = -(1 - \beta) \int \int_v \bar{Q}_{16} \eta^2 dA - d_1 \int \int_{h,v} \bar{Q}_{12} \eta^2 dA \quad [A11]$$

$$K_{55} = \int \int_{h,v} \bar{Q}_{11} \zeta^2 dA - c_2 \int \int_{h,v} \bar{Q}_{12} \zeta^2 dA \quad [A12]$$

$$K_{66} = \int \int_{h,v} \bar{Q}_{11} \eta^2 dA - b_1 \int \int_{h,v} \bar{Q}_{12} \zeta^2 dA \quad [A13]$$

These stiffness parameters contain a number of constants such as  $a_0$ ,  $b_1$ ,  $c_2$ , etc. These constants arise from the refined treatment of the two-dimensional in-plane elastic behavior. The constants are defined by the expressions given below

$$a_0 = - \frac{\int \int_{h,v} \bar{Q}_{12} dA}{\int \int_{h,v} \bar{Q}_{22} dA} \quad [A14]$$

$$b_1 = \frac{\int \int_{h,v} \bar{Q}_{12} \eta^2 dA}{\int \int_{h,v} \bar{Q}_{22} \eta^2 dA} \quad [A15]$$

$$c_2 = \frac{\int \int_{h,v} \bar{Q}_{12} \zeta^2 dA}{\int \int_{h,v} \bar{Q}_{22} \zeta^2 dA} \quad [A16]$$

$$d_0 = \frac{(1+\beta) \int \int_h \bar{Q}_{26} \zeta dA - (1-\beta) \int \int_v \bar{Q}_{26} \eta dA}{\int \int_{h,v} \bar{Q}_{22} dA} \quad [A17]$$

$$d_1 = - \frac{(1-\beta) \int \int_v \bar{Q}_{26} \eta^2 dA}{\int \int_{h,v} \bar{Q}_{22} \eta^2 dA} \quad [A18]$$

$$d_2 = \frac{(1+\beta) \int \int_h \bar{Q}_{26} \zeta^2 dA}{\int \int_{h,v} \bar{Q}_{22} \zeta^2 dA} \quad [A19]$$

$$f_0 = - \frac{\int \int_h \bar{Q}_{26} dA}{\int \int_h \bar{Q}_{22} dA} \quad [A20]$$

$$f_2 = - \frac{\int \int_h \bar{Q}_{26} \zeta dA}{\int \int_h \bar{Q}_{22} dA} \quad [A21]$$

$$g_0 = - \frac{\int \int_v \bar{Q}_{26} dA}{\int \int_v \bar{Q}_{22} dA} \quad [A22]$$

$$g_1 = - \frac{\int \int_v \bar{Q}_{26} \eta dA}{\int \int_v \bar{Q}_{22} dA} \quad [A23]$$

## Appendix B. Special Forms of Governing Equations

### Cross-Ply Layup

This configuration has no elastic couplings.

$$\begin{Bmatrix} F \\ Q_y \\ Q_z \end{Bmatrix} = \begin{bmatrix} K_{11} & 0 & 0 \\ 0 & K_{22} & 0 \\ 0 & 0 & K_{33} \end{bmatrix} \begin{Bmatrix} u' \\ \gamma_{xy}^0 \\ \gamma_{xz}^0 \end{Bmatrix} \quad [B1]$$

$$\begin{Bmatrix} T \\ M_y \\ M_z \end{Bmatrix} = \begin{bmatrix} K_{44} & 0 & 0 \\ 0 & K_{55} & 0 \\ 0 & 0 & K_{66} \end{bmatrix} \begin{Bmatrix} \phi' \\ w'' - \gamma_{xy}^{0'} \\ v'' - \gamma_{xz}^{0'} \end{Bmatrix} \quad [B2]$$

### Symmetric Layup

This configuration displays bending-torsion coupling and extension-shear couplings.

$$\begin{Bmatrix} F \\ Q_y \\ Q_z \end{Bmatrix} = \begin{bmatrix} K_{11} & K_{12} & K_{13} \\ K_{12} & K_{22} & 0 \\ K_{13} & 0 & K_{33} \end{bmatrix} \begin{Bmatrix} u' \\ \gamma_{xy}^o \\ \gamma_{xz}^o \end{Bmatrix} \quad [B3]$$

$$\begin{Bmatrix} T \\ M_y \\ M_z \end{Bmatrix} = \begin{bmatrix} K_{44} & K_{45} & K_{46} \\ K_{45} & K_{55} & 0 \\ K_{46} & 0 & K_{66} \end{bmatrix} \begin{Bmatrix} \phi' \\ w'' - \gamma_{xy}^{o'} \\ v'' - \gamma_{xz}^{o'} \end{Bmatrix} \quad [B4]$$

Note that the bending and torsion of the beam is not elastically coupled to the extension and shearing of the beam.

### Anti-Symmetric Layup

This configuration displays extension-torsion coupling and bending-shear couplings.

$$\begin{Bmatrix} F \\ T \end{Bmatrix} = \begin{bmatrix} K_{11} & K_{14} \\ K_{14} & K_{44} \end{bmatrix} \begin{Bmatrix} u' \\ \phi' \end{Bmatrix} \quad [B5]$$

$$\begin{Bmatrix} Q_y \\ Q_z \\ M_y \\ M_z \end{Bmatrix} = \begin{bmatrix} K_{22} & 0 & K_{25} & 0 \\ 0 & K_{33} & 0 & K_{36} \\ K_{25} & 0 & K_{55} & 0 \\ 0 & K_{36} & 0 & K_{66} \end{bmatrix} \begin{Bmatrix} \gamma_{xy}^o \\ \gamma_{xz}^o \\ w'' - \gamma_{xy}^{o'} \\ v'' - \gamma_{xz}^{o'} \end{Bmatrix} \quad [B6]$$

Note that the extension and torsion of the beam is not elastically coupled to the bending and shearing of the beam.

## Appendix C. Effects of Shear Couplings on Beam Compliance

### Symmetric Layup

If an axial force,  $F$ , is applied to a symmetric layup uniform box-beam, then the resulting axial

deformation can be determined from matrix inversion to be

$$u' = \frac{F}{K_{11} \left[ 1 - \frac{(K_{12})^2}{K_{11}K_{22}} - \frac{(K_{13})^2}{K_{11}K_{33}} \right]} \quad [C1]$$

Note the effective increase in axial compliance due to the extension-shear couplings  $K_{12}$  and  $K_{13}$ . This increase is independent of the length of the beam. The magnitude of the increase depends on cross-section geometry and on the composite design of the beam walls. The primary design parameters are material selection, ply orientation angles, and stacking sequence.

It is also important to note that the axial deformation will be accompanied by shearing deformations due to the extension-shearing coupling mechanism.

### Anti-Symmetric Layup

If a transverse bending force is applied to a anti-symmetric layup uniform box-beam, by application of loads  $Q_z$  and  $M_y$ , then the resulting deflection can be determined from matrix inversion to be

$$w'' = \frac{Q_z'}{K_{33} \left[ 1 - \frac{(K_{36})^2}{K_{33}K_{66}} \right]} + \frac{M_y}{K_{55} \left[ 1 - \frac{(K_{25})^2}{K_{22}K_{55}} \right]} \quad [C2]$$

The first term is the shear component of the deflection and the second term is the bending component of the deflection. Note the effective increase in bending compliance due to the bending-shear coupling  $K_{25}$ . Once again, this increase is independent of the length of the beam. The magnitude of the increase depends on cross-section geometry and on the composite design of the beam walls.

It is also interesting to note that some degree of shearing and bending will occur perpendicular to the applied direction of loading. This behavior is caused by the bending-shearing coupling mechanism.